

Impact of symbol transition density on timing estimation

Jaume Riba¹

Signal Processing and
Communications group.

Technical University of Catalonia
(UPC)

Jordi Girona 1-3, Campus Nord,
Ed. D5, 08034, Barcelona, SPAIN

Email: jriba@gps.tsc.upc.es

Abstract — **The symbol transition density in a digitally modulated signal affects the performance of practical synchronization schemes designed for timing estimation. This paper focuses on the derivation of a simple performance limit for the estimation of the time delay of a noisy linearly modulated signal in the presence of various degrees of symbol correlation produced by the various transition densities in the symbol streams. The approach relies on the (Gaussian) Unconditional Cramer-Rao Bound (UCRB), well known in the array signal processing literature. The derived bound is valid only for the class of quadratic, Non-Data-Aided (NDA) timing recovery schemes, but it becomes asymptotically the true CRB for low-SNR. To illustrate the validity of the derive bound, it is compared with the actual performance achieved by some well-known quadratic NDA timing recovery schemes.**

I. INTRODUCTION

Non-Data-Aided (NDA) timing recovery schemes have the important ability of extracting the timing directly from the noisy digital waveform, without the use of symbol decisions. The achievable Bit-Error-Rate (BER) is affected by the resulting timing variance, mainly in low Signal-to-Noise-Ratio (SNR) conditions. Cramer-Rao-Bounds (CRB) are of common use for a prior evaluation of the this variance, but the exact CRB for timing has not a simple closed-form expression. The use of the Modified CRB (MCRB) [1] is an option, but it may yield too much optimistic values. Another option is to use low-SNR approximations of the CRB, as that obtained in [2].

The present contribution tries to give some answers to the following questions: a) how the symbol transition density impacts on the timing accuracy? b) how to know in advance whether a particular working SNR can be considered low enough to apply the existing low-SNR approximations?

The importance of question a) comes from the fact that in some applications, such as Earth-to-space links, the data stream may not be coded in order to simplify the equipment on board the spacecraft, and adequate transitions cannot be assured. Question a) becomes also an important in the contrary sense: to which extent the use of alternated patterns with high symbol transition densities may help the timing recovery? Concerning

question b) we are interested in knowing when a low-SNR approximation is valid for a given SNR working point, and if this depends also on the actual symbol transition density.

In the present contribution, we basically derive a simple CRB expression from which the result in [2] is obtained as a particular case. The general expression derived here takes into account both the actual symbol transition density and the actual SNR. For low-SNR, the expression becomes the true CRB, while in the whole range of SNR, the expression has to be understood as a performance limit only for quadratic estimators. Note that most simple NDA feedback schemes for timing recovery are quadratic systems, and therefore the obtained expression is valid at any SNR whenever this class of estimators is chosen. The starting point resorts on the theory presented in [3], where the use of the so-called Gaussian Unconditional CRB (UCRB) is proposed for synchronization. The reader is referred to the excellent work about the UCRB under the scope of sensor array processing, as [8] and [7], for further details.

II. BACKGROUND: THE UNCONDITIONAL CRB APPLIED TO TIMING RECOVERY

The complex base-band signal is represented as:

$$r(t) = e^{j\theta} \sum_{k=0}^{L-1} a_k g(t - kT - \tau) + w(t) \quad (1)$$

where τ is the timing parameter to be estimated, θ is the signal phase, $\{a_k\}$ are zero-mean complex-valued stationary data symbols with autocorrelation $r_a[p] = E[a_k a_{k+p}^*]$ and pertaining to the alphabet $a_k \in a^{(n)}$ ($n = 0, \dots, N-1$) where N is the alphabet size, T is the symbol interval, $g(t)$ is a real-valued signalling pulse, and $w(t)$ is complex-valued zero-mean Gaussian noise with independent real and imaginary parts, each one having a power spectral density of N_o . In the above model (1), L represents the number of symbols considered in the observation interval that will be used for timing estimation. The symbol energy of the modulated passband signal is defined as $E_s = \sigma_a^2 E_g / 2$, with E_g is the pulse energy, where $\sigma_a^2 = r_a[0]$. By sampling $r(t)$ at intervals $T_s = T/N_{ss}$, where N_{ss} is the number of samples per symbol, and assuming that the sampling frequency $F_s = 1/T_s$ is above the Nyquist frequency, a discrete model can be used for $r(t)$ as follows [4][3]:

$$\mathbf{r} = \mathbf{A}_\tau \mathbf{x} + \mathbf{w} \quad (2)$$

where \mathbf{r} is the sampled signal vector, the k -th column of matrix \mathbf{A}_τ is formed by the samples of $g(t - kT - \tau)$, $\mathbf{x} = e^{j\theta} [a_0, a_1, \dots, a_{L-1}]^T$ with covariance $\mathbf{\Gamma}$, and \mathbf{w} is the noise

¹This work has been partially supported by the following research projects of the Spanish/Catalan Science and Technology Commissions (CICYT/CIRIT): TIC2003-05482, TIC2002-04594, TIC2001-2356, TIC2000-1025 and 2001SGR-00268.

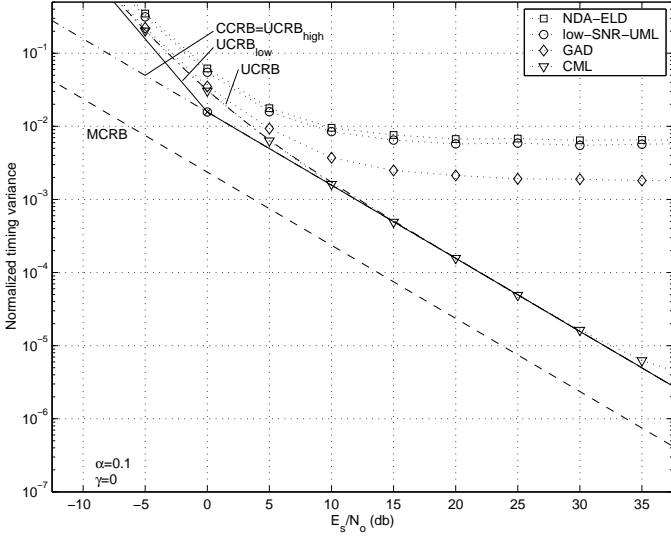


Figure 1: σ_τ^2/T^2 for BPSK with $L = 64$, $\alpha = 0.1$ and 50% transition density (uncorrelated symbols).

vector of covariance $\mathbf{C}_w = \sigma^2 \mathbf{I}$, where $\sigma^2 = 2N_o/T_s$. For simplicity the paper is focused only to the case of pulses that do not generate intersymbol interference (ISI) at the matched filter output, which means that $T_s \mathbf{A}_\tau^T \mathbf{A}_\tau = E_g \mathbf{I}$. The Gaussian Unconditional CRB (UCRB) for the parameter τ can be applied to (2) to yield:

$$UCRB(\tau) = \frac{\sigma^2}{2\text{tr}(\mathbf{Y}\mathbf{S})} \quad (3)$$

where

$$\begin{aligned} \mathbf{Y} &= \mathbf{D}_\tau^T \mathbf{P}_{\mathbf{A}_\tau}^\perp \mathbf{D}_\tau \\ \mathbf{S} &= \mathbf{\Gamma} \mathbf{A}_\tau^T \mathbf{R}_\tau^{-1} \mathbf{A}_\tau \mathbf{\Gamma} \\ \mathbf{R}_\tau &= \mathbf{A}_\tau \mathbf{\Gamma} \mathbf{A}_\tau^T + \sigma^2 \mathbf{I} \\ \mathbf{P}_{\mathbf{A}_\tau}^\perp &= \mathbf{I} - \frac{T_s}{E_g} \mathbf{A}_\tau \mathbf{A}_\tau^T \\ \mathbf{D}_\tau &= d\mathbf{A}_\tau/d\tau \end{aligned}$$

where the k -th column of matrix \mathbf{D}_τ is formed by the samples of $g'(t - kT - \tau)$, and $g'(t) = d g(t)/dt$. For more information about the validity of this bound for synchronization, the reader is referred to [3]. In short, we just mention that (3) applies only to the set of quadratic timing estimators, and it becomes asymptotically the true CRB for low SNR (see [7] for more details).

III. DERIVATION OF A MEANINGFUL EXPRESSION

Through matrix inversion lemma, it is not difficult to show [5] that $\mathbf{S} = \mathbf{\Gamma} \mathbf{\Omega}^{-1} \mathbf{\Gamma}$, where $\mathbf{\Omega} = \mathbf{\Gamma} + \sigma^2 (\mathbf{A}_\tau^T \mathbf{A}_\tau)^{-1}$. Then, the term $\text{tr}(\mathbf{Y}\mathbf{S})$ in (3) for large L can be expressed as¹:

$$\begin{aligned} \text{tr}(\mathbf{Y}\mathbf{S}) &= \text{tr}(\mathbf{Y}\mathbf{\Gamma}\mathbf{\Omega}^{-1}\mathbf{\Gamma}) \\ &= L \int_{-1/2}^{1/2} Y(F) R_a(F) \mathbf{\Omega}^{-1}(F) R_a(F) dF \end{aligned} \quad (4)$$

¹See [4], appendix B, Proposition B.3, for a detailed proof of (4).

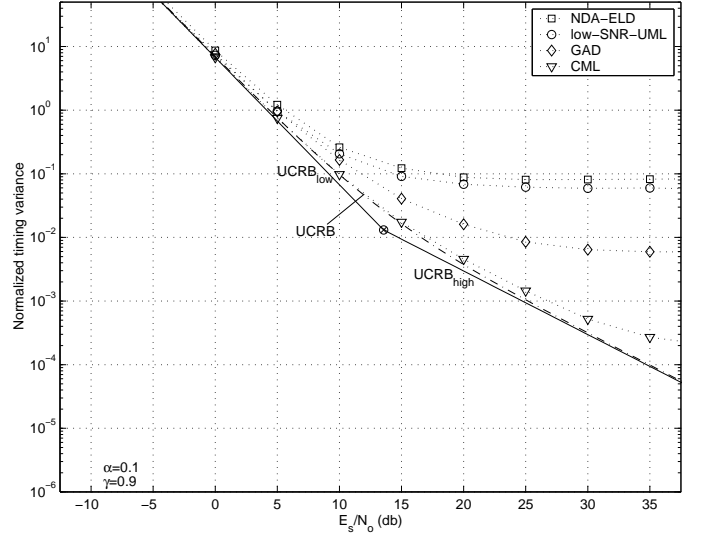


Figure 2: σ_τ^2/T^2 for BPSK with $L = 64$, $\alpha = 0.1$ and 5% transition density.

where:

$$\begin{aligned} Y(F) &= \sum_{p=-\infty}^{\infty} y[p] e^{-j2\pi Fp} \\ R_a(F) &= \sum_{p=-\infty}^{\infty} r_a[p] e^{-j2\pi Fp} \\ \mathbf{\Omega}(F) &= R_a(F) + \frac{\sigma^2 T_s}{E_g} \end{aligned}$$

where $y[p]$ and $r_a[p]$ are the common element of the p -th diagonal of Toeplitz matrices \mathbf{Y} and $\mathbf{\Gamma}$ respectively. More compactly we can write:

$$\text{tr}(\mathbf{Y}\mathbf{S}) = L \int_{-1/2}^{1/2} Y(F) S_a(F) dF \quad (5)$$

where:

$$S_a(F) = \frac{|R_a(F)|^2}{R_a(F) + \frac{\sigma^2 T_s}{E_g}} = \sigma_a^2 \frac{|\bar{R}_a(F)|^2}{\bar{R}_a(F) + \left(\frac{E_s}{N_o}\right)^{-1}} \quad (6)$$

with $\bar{R}_a(F)$ the normalized discrete Fourier transform of $r_a[p]$ defined as $\bar{R}_a(F) = \frac{1}{\sigma_a^2} R_a(F)$. Now, defining $s_a[p] = \int_{-1/2}^{1/2} S_a(F) e^{j2\pi Fp} dF$, which can be numerically computed in practice by means of the IFFT algorithm, we can use the Parseval's theorem to write:

$$\text{tr}(\mathbf{Y}\mathbf{S}) = L \sum_{p=-\infty}^{\infty} y[p] s_a[p] \quad (7)$$

Matrix \mathbf{Y} can be written as:

$$\mathbf{Y} = \mathbf{D}_\tau^T \mathbf{P}_{\mathbf{A}_\tau}^\perp \mathbf{D}_\tau = \mathbf{D}_\tau^T \mathbf{D}_\tau - \frac{T_s}{E_g} \mathbf{B}_\tau^T \mathbf{B}_\tau \quad (8)$$

where:

$$\mathbf{B}_\tau = \mathbf{A}_\tau^T \mathbf{D}_\tau \quad (9)$$

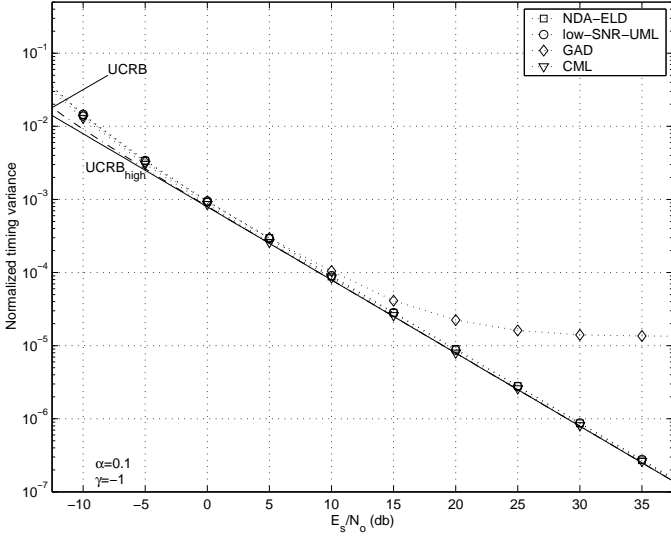


Figure 3: σ_τ^2/T^2 for BPSK with $L = 64$, $\alpha = 0.1$ and 100% transition density.

Matrices $\mathbf{D}_\tau^T \mathbf{D}_\tau$ and \mathbf{B}_τ are $L \times L$ Toeplitz and their diagonals have a common element that can be easily related with the following cross-correlation functions:

$$\overline{\text{diag}}_p [\mathbf{D}_\tau^T \mathbf{D}_\tau] = r_{g'}(pT)/T_s = -r_g''(pT)/T_s \quad (10)$$

$$\overline{\text{diag}}_p [\mathbf{B}_\tau] = r_{gg'}(pT)/T_s = r_g'(pT)/T_s \quad (11)$$

where $r_g(\tau) = \int g(t)g(t+\tau)dt$, $r_{gg'}(\tau) = \int g(t)g'(t+\tau)dt$, $r_{g'}(\tau) = \int g'(t)g'(t+\tau)dt$, $r_g'(\tau) = d r_g(\tau)/d\tau$, $r_g''(\tau) = d^2 r_g(\tau)/d\tau^2$, and $\overline{\text{diag}}_p$ represents the common element of the p th diagonal ($p = -(L-1), \dots, 0, \dots, L-1$) of a Toeplitz matrix. On the other hand, we have approximately that:

$$T_s^2 \overline{\text{diag}}_p [\mathbf{B}_\tau^T \mathbf{B}_\tau] \approx q_g[p] = \sum_{m=-\infty}^{\infty} r_g'(mT)r_g'((m+p)T) \quad (12)$$

Then, the coefficients $y[p]$ (the diagonals of \mathbf{Y}) can be written as:

$$y[p] = \frac{1}{T_s} \left(-r_g''(pT) - \frac{1}{E_g} q_g[p] \right) \quad (13)$$

Substituting (13) in (3), we can write:

$$\begin{aligned} UCRB(\tau) &= \frac{\sigma_a^2 T_s}{2LS} = \frac{N_o}{LS} \quad (14) \\ S &= \sum_{p=-\infty}^{\infty} \left(-r_g''(pT) - \frac{1}{E_g} q_g[p] \right) s_a[p] \end{aligned}$$

Finally, straightforward manipulation of (14) yields the main result of this paper, generalizing [2]:

$$UCRB(\tau) = \frac{1}{2L} \frac{1}{E_s/N_o} \frac{\sigma_a^2 E_g}{\sum_{p=-\infty}^{\infty} \left(-r_g''(pT) - \frac{1}{E_g} q_g[p] \right) s_a[p]} \quad (15)$$

IV. PARTICULAR CASES

For the particular case of uncorrelated data, the coefficients $s_a[p]$ (the inverse Fourier transform of $S_a(f)$ in (6) for $\overline{R}_a(F) = 1$) in (15) reduce to:

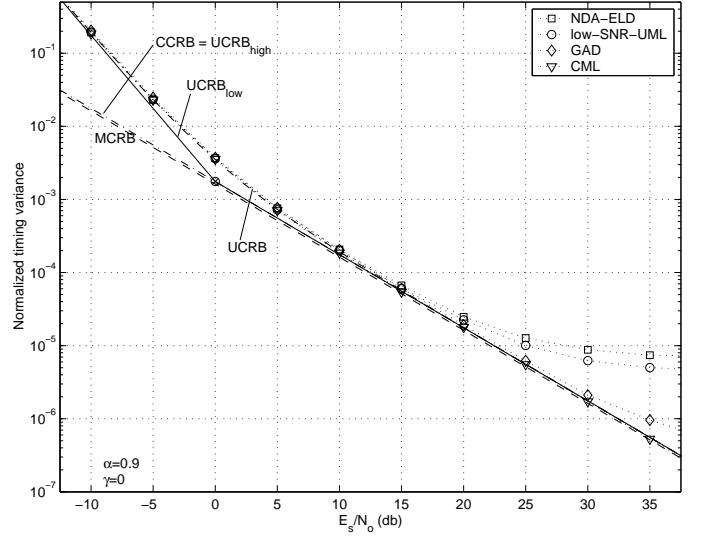


Figure 4: σ_τ^2/T^2 for BPSK with $L = 64$, $\alpha = 0.9$ and 50% transition density (uncorrelated symbols).

$$s_a[p] = \sigma_a^2 \frac{E_s/N_o}{E_s/N_o + 1} \delta_p \quad (16)$$

where δ_p is the Kronecker delta. In addition, taking into account from (12) that $q_g[0] = \sum_{m=-\infty}^{\infty} r_g'^2(mT)$, we obtain:

$$UCRB_u(\tau) = \frac{1}{2L} \frac{1 + \frac{1}{E_s/N_o}}{E_s/N_o} \frac{E_g}{-r_g''(0) - \frac{1}{E_g} \sum_{m=-\infty}^{\infty} r_g'^2(mT)} \quad (17)$$

Finally, for $E_s/N_o \ll 1$ we obtain from (17) the low-SNR limit derived in [2]:

$$UCRB_{ul}(\tau) = \frac{1}{2L} \frac{1}{(E_s/N_o)^2} \frac{E_g}{-r_g''(0) - \frac{1}{E_g} \sum_{m=-\infty}^{\infty} r_g'^2(mT)} \quad (18)$$

V. SIMULATION RESULTS

The derived performance bound (15) is here compared with the actual performance of some well-known quadratic timing recovery feed-back schemes in the presence of uncorrelated and correlated data. Four timing error detectors are considered: the Non-Data-Aided Early-Late detector (NDA-ELD) (see [6], Sec. 8.3.1., pag. 429, Eq. 8.3.7.), the low-SNR-UML (or ML-oriented) detector (see [4][3]), the Gardner detector (GAD) (see [6], Sec. 8.3.2., pag 431, Eq. 8.3.19) and the CML detector (see [4]). Figures (1) to (3) show the normalized timing variance of all timing error detectors against E_s/N_o using 5000 iterations with $L = 64$, along with the UCRB and their asymptotic limits.

Figure (1) corresponds to the case of uncorrelated data. It is seen that only the CML detector attains the UCRB (for moderate E_s/N_o). The remaining detectors exhibit a very high floor effect for this small roll-off factor, α . The MCRB is also depicted, which departs significantly from the UCRB. Figure (2) corresponds to the case of a low transition density. The simulations show the existence of an increased threshold effect for that case, approaching all the estimators to the $UCRB_{low}$ asymptote below this threshold. The case of 100% transition density is shown in figure (3) where, apart from the GAD, the detectors

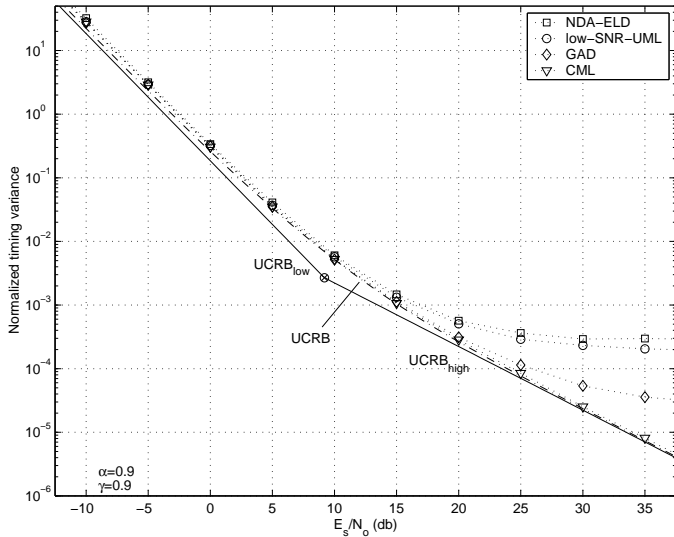


Figure 5: σ_τ^2/T^2 for BPSK with $L = 64$, $\alpha = 0.9$ and 5% transition density.

attain the UCRB for moderate and high E_s/N_o and they exhibit a reduced threshold effect. However, all them tend to depart slightly from the UCRB at very low E_s/N_o .

Figures (4), (5) and (6), are similar to figures (1), (2) and (3), respectively, but for the case of a high roll-off factor. The floor effect of all estimators is smaller in that case. In figure (4), all the detectors attain the UCRB, except those affected by self noise, which exhibit a floor for high E_s/N_o . The MCRB is also depicted, which is very near to the $UCRB_{high}$ asymptote for roll-off factors near to 1. Figure (5) shows again threshold effect correctly predicted by the bound, which is a little smaller in that case, in comparison with that in figure (2). Finally, in the case of 100% transition density shown in figure (6) all detectors attain the UCRB at high E_s/N_o . However, for this case of alternated pattern and roll-off factor near to 1, it is seen that they depart more significantly from the UCRB at small E_s/N_o , which means that they have a threshold value higher than that predicted by the bound. With the purpose of validating the obtained result by showing that an estimator exists near the bound, an additional ad-hoc quadratic timing detector described in [5] has been considered in figure (6), which has been named High Transition Density NDA-ELD (HTD-NDA-ELD). The message behind this simulation is that, at low-SNR it is necessary to make modifications to the estimator in order to attain the bound in the presence of high transition density, mainly for high roll-off factors.

VI. SUMMARY AND CONCLUSIONS

In this paper we have analyzed the effect of symbol transition density on timing estimation, resorting to the so-called Unconditional CRB, well known in array signal processing. The results show the existence of a threshold E_s/N_o at which the slope of the UCRB changes from -2dB per dB to -1dB per dB. This threshold increases above 0dB for low transition densities, while it decreases below 0dB for high transition densities, which indicates that the use of alternated symbol patterns is specially attractive only for very low SNR. The already existing low-SNR limit for timing recovery for uncorrelated data [2] is obtained

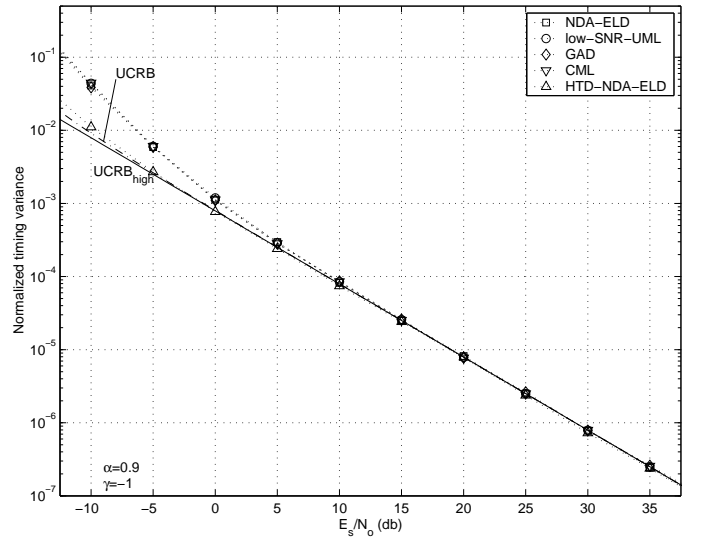


Figure 6: σ_τ^2/T^2 for BPSK with $L = 64$, $\alpha = 0.9$ and 100% transition density.

as a special case by using the proposed approach. The bound is also useful for knowing in advance whether modifications to the estimator will be worth for improving the performance.

The research is extended in [5], where even simpler expressions are derived for the high and low-SNR asymptotes of the UCRB, which also allows the derivation of a closed-form expression for the threshold E_s/N_o .

REFERENCES

- [1] Aldo D'Andrea, Umberto Mengali and Ruggero Reggiannini, "The modified Cramer-Rao bound and its application to synchronization problems", *IEEE Transactions on Communications*, 42(2/3/4), pp. 1391-1399, February/March/April, 1994.
- [2] Heidi Steendam and Marc Moeneclaey, "Low-SNR Limit of the Cramer-Rao bound for estimating the time delay of a PSK, QAM, or PAM waveform", *IEEE Communications Letters*, 5(1), pp. 31-33, January, 2001.
- [3] Gregori Vazquez and Jaume Riba, "Non-Data-Aided digital synchronization", *Signal Processing Advances in Wireless and Mobile Communications*, by G. B. Giannakis, Y. Hua, P. Stoica and L. Tong, volume 2 (Trends in Single and Multi-User Systems), chapter 9, Prentice Hall, July 2000.
- [4] Jaume Riba, Josep Sala and Gregori Vazquez, "Conditional maximum likelihood timing recovery: estimators and bounds", *IEEE Transactions on Signal Processing*, 49(4), pp. 835-850, April, 2001.
- [5] Jaume Riba, "A performance lower bound for quadratic timing recovery accounting for the symbol transition density", *IEEE Transactions on Signal Processing*, accepted for publication, 2004.
- [6] Umberto Mengali and Aldo D'Andrea, "Synchronization techniques for digital receivers", Plenum Press, 1997.
- [7] B. Ottersten, M. Viberg and T. Kailath, "Analysis of subspace fitting and ML techniques for parameter estimation from sensor array data", *IEEE Transactions on Signal Processing*, 40(3), pp. 590-600, March, 1992.
- [8] Petre Stoica and Arye Nehorai, "Performance study of conditional and unconditional direction-of-Arrival Estimation", *IEEE Transactions on Acoustics, Speech and Signal Processing*, 38(10), pp. 1783-1795, October, 1990.